Title: A novel microfluidic-based approach to formulate size-tuneable large unilamellar cationic liposomes: formulation, cellular uptake and biodistribution investigations.

Authors: Gustavo Lou, Giulia Anderluzzi, Stuart Woods, Craig W. Roberts and Yvonne Perrie

Strathclyde Institute of Pharmacy and Biomedical Sciences, University of Strathclyde, Glasgow, Scotland.

Key Words: Microfluidics, cationic liposomes, liposome size, macrophage uptake, biodistribution, particle size.

Corresponding author:

Professor Yvonne Perrie

Strathclyde Institute of Pharmacy and Biomedical Sciences,

161 Cathedral St,

University of Strathclyde,

Glasgow, G4 0RE

Scotland.

yvonne.perrie@strath.ac.uk

Abstract

Extensive research has been undertaken to investigate the effect of liposome size *in vitro* and *in vivo*. However, it is often difficult to generate liposomes in different size ranges that offer similar low polydispersity and lamellarity. Conventional methods used in the preparation of liposomes, such as lipid film hydration or reverse phase evaporation, generally give rise to liposomal suspensions displaying broad, multimodal size distribution combined with uncontrolled degree of lamellarity. In contrast, microfluidics allows highly homogeneous liposome dispersions to be produced and adjustment of microfluidic operating parameters (flow rate ratio (FRR) and total flow rate (TFR)) can offer size-tuning of liposomes (up to 300 nm, depending on the formulation). Herein, we demonstrate a novel method which allows the production of highly monodisperse, cationic liposomes over a wide particle size range (up to 750 nm in size). This is achieved through controlling the concentration of the aqueous buffer during production. Using this method, liposomes composed of 1,2-dioleoyl-sn-3-phosphoethanolamine (DOPE) and 1,2-dioleoyl-3-trimethylammonium-propane (DOTAP) or dimethyldioctadecylammonium (DDA) – DOPE:DOTAP and DOPE:DDA liposomes – of up to 750 nm were prepared and investigated. Investigating these formulations *in vitro* demonstrates that cellular uptake of small (40 nm) and large (>500 nm) liposomes in bone marrow-derived macrophages (BMDM) is similar terms of percentage of liposome$^+$ cells and mean fluorescence intensity (MFI). However, significant differences are observed in BMDM uptake when represented in terms of number of liposomes, liposome surface area or liposome internal volume. *In vivo* biodistribution studies in mice show that by creating small (<50 nm) liposomes we can modify the clearance rates of these liposomes from the injection site and increase accumulation to the draining lymphatics.

Introduction

Since their discovery in 1965 [1], liposomes are widely reported for their use as drug delivery systems and, more recently, in their use for delivery of sub-unit [2] and nucleic acid based vaccines [3, 4]. Commonly, liposomes are produced by the lipid film hydration method developed by Bangham [1]. This method gives rise to multilamellar vesicles (MLVs) of several hundred nanometers in size with a broad size distribution. Because it is based on the macroscopic mixing of organic and aqueous phases, it also offers poor batch-to-batch reproducibility. Consequently, size reduction techniques (e.g. extrusion or probe sonication) are often required. Although homogeneous liposome dispersions with relatively narrow size distribution can be obtained, scaling-up these methods can be challenging. Furthermore, to achieve a homogeneous liposome suspension, generally particle size reduction to below 100 nm is required, and it is difficult to form homogenous populations of larger liposome systems using these methods. Ethanol injection is another popular technique for producing large unilamellar liposomes that consists of rapidly injecting an ethanol solution containing lipids into an aqueous phase [5]. However, this method is not easy to translate to large scale and is more commonly used for the production of small unilamellar vesicles (SUV).

In contrast to these methods, microfluidic-based techniques not only enable reliable laminar flow dynamics [6] and thus robust liposome formulation, but also ease of scale-up [7]. Moreover, microfluidic-based techniques promote effective incorporation of both hydrophilic and hydrophobic drugs simultaneously, with higher encapsulation efficiencies compared to conventional techniques [8]. A range of studies has been undertaken to understand how the microfluidics operating parameters affect the physicochemical attributes of liposomes, especially size and size distribution. These parameters usually include aqueous:organic flow rate ratio (FRR), total flow rate (TFR) and lipid concentration. However, other variables should be taken into consideration, including micromixer design (geometry, microchannel size, orientation of inlet channels) and liposome composition. For example, Jahn et al. made use of microfluidic hydrodynamic focusing (MHF) cartridges of 10 and 65 µm width to demonstrate that the combination of micromixer geometry and hydrodynamic flow focusing regime had an impact on liposome size [9]. Based on current research, FRR is one of the most important parameters to consider when formulating liposomes by microfluidics [10]. Indeed, liposome formation in the micromixer is promoted by the mixing between organic and aqueous phases, which makes the lipids nanoprecipitate and self-assemble into planar lipid bilayers, which bend to reduce contact of the hydrophobic acyl chains of the lipids with the water phase, and eventually close into spherical vesicles. The higher the FRR, the more rapidly the concentration of alcohol will decrease and the less the time for lipids discs to stabilize. Therefore, smaller liposomes are expected at increasing FRR [10]. The same trend was observed by Jahn et al. in their studies [9, 11]. On the other hand, TFR

has been reported to have little to no effect on liposome size [8, 12-14]. However, current research with microfluidics have demonstrated the ability to produce small homogeneous unilamellar vesicle systems and the methodology has not been exploited to consider larger liposomal systems.

As first described by Israelachvili [15], the geometry in which lipids self-assemble is given by the critical packing parameter of the lipids (P_C). P_C is defined as $v/a_0 \cdot l_c$, where a_0 is the effective area of the head group, l_c is the length of the alkyl chain and v is the alky chain volume. Therefore, P_C can be used to predict what structural aggregates the lipids will form [16]. For $P_C \leq 1$, lamellar (L_α) phases are formed, including spherical micelles ($P_C < 0.3$), worm-like micelles ($P_C = 1/3 – 1/2$), vesicles ($P_C = 1/2 – 1$) and planar bilayers ($P_C \sim 1$), For $P_C > 1$, inverted hexagonal (H_{II}) and cubic phases (Q_{II}) appear. For charged lipids, the presence of electrolytes can potentially reduce the repulsion among lipid head groups, reducing a_0 and consequently increasing P_C. From this point of view, we have investigated the use of microfluidics to produce liposomes in a range of sizes (40 – 750 nm) and we hypothesized that increasing the ionic strength of the aqueous phase (i.e. buffer concentration) used in microfluidics could increase lipid P_C enough to form cationic large unilamellar liposomes but not enough to induce a negative curvature and the consequent formation of non-liposomal self-assemblies such as cubosomes.

The ability to produce size-tuned liposomes over a large size range can provide new opportunities to investigate and exploit liposomal drug delivery systems given their suitability as drug and vaccine delivery systems is heavily dependent on their physicochemical properties, including surface charge [17], size [18, 19], hydrophobicity/hydrophilicity [20] and lamellarity [21]. In particular, both the liposome size and surface charge are recognised as important parameters that can influence their cellular uptake and biodistribution. However, there remains a lack of clarity when considering the role of size coupled with charge in relation to the function of liposomal systems and current manufacturing methods have limited our ability to effectively explore this issue. For example, a relationship between *in vitro* cellular uptake and liposome surface charge has been shown, with charged (anionic and cationic) liposomes being better internalized than neutral ones [22, 23]. Additionally, increasing percentages of charged lipid within the formulation enhances cellular uptake [24, 25]. It has been also reported that increasing the size of anionic liposomes from 80 nm up to 600 nm initially increases cellular uptake but by 48 h uptake was similar across all size ranges [22] In contrast, studies using neutral liposomes have shown the opposite effect. Work by Andar et al [26] investigated the cellular uptake mechanisms of neutral liposomes prepared by microfluidics. In their studies, the authors investigated sizes ranges of 40 to 275 nm and show liposome uptake is strongly size dependent, with smaller liposomes showing higher uptake and that the uptake mechanisms also varying with size [26]. In further contrast to this, with cationic formulations we have previously shown the vesicle size has

no impact on cellular uptake [27] although in these studies the smallest size investigated was approximately 200 nm.

When considering the effect of surface charge and size on the *in vivo* fate of liposomes, again we see the two factors must be considered in combination. For example, cationic liposomes are retained longer at the injection site compared to neutral formulations when administered intramuscularly [27, 28] or subcutaneously [17, 29]. Furthermore, clearance of the cationic liposomes from the injection site was not influenced by particle size when considering particle size ranges from approximately 200 to 3000 nm [27]. In contrast, anionic liposomes do not aggregate upon injection and can drain to the local lymph nodes with SUV showing a more rapid drainage compared to MLV [30]. These differences are due to aggregation of the cationic vesicles in the presence of proteins found within the extracellular matrix at the injection site. These electrostatic interactions resulting from the cationic nature of the liposomes was shown to be more important than the size of the vesicles in terms of clearance from the injection site [20, 28]. These electrostatic interactions at the injection site can be avoided by masking the cationic nature of the liposomes via PEGylation; in the case of liposomes composed of dimethyldioctadecylammonium bromide (DDA) and trehalose 6,6'-dibehenate (TDB) incorporation of 25 mol% PEG was required to block the depot effect and promote drainage to the local lymph node irrespective of the size of the liposomes (120 nm up to 500 nm) [28] and resulted in different immune response profiles [20]. Indeed with anionic vesicles, the particle size has been shown to play a major role in the intracellular trafficking, processing and presentation of antigens by antigen presenting cells [31] and dictates the type of immune responses. For instance, in a study conducted by Brewer et al., liposomes above 225 nm generated IgG2a titers and high production of IFN-γ, characteristic pattern of a Th1 response. In contrast, smaller liposomes (<155 nm) induced a Th2 responses, as evidenced by production of IgG1 and IL-5 [19] In another study, 100 nm liposomes induced a Th2 response, while 400 and 1000 nm liposomes induced Th1 type immune responses [32]

However, in many of these studies size reduction techniques were used to produce the different particle size populations and thus lamellarity cannot easily be controlled/standardised; with larger vesicles being multilamellar in nature compared to the lower size ranges unilamellar vesicles. Therefore, the aim of work outlined was to develop a new microfluidic process to prepare cationic SUV and large unilamellar vesicles (LUV) using a size-tuning process and to use this methodology to compare the uptake and biodistribution of cationic liposomal systems.

Materials and Methods

Materials

1,2-dioleoyl-sn-3-phosphoethanolamine (DOPE), 1,2-dioleoyl-3-trimethylammonium-propane (DOTAP), dimethyldioctadecylammonium (DDA) and 1,2-distearoyl-sn-glycero-3-phosphocholine (DSPC) were obtained from Avanti Polar Lipids. The fluorescent dye 1,1'-Dioctadecyl-3,3,3',3'-Tetramethylindocarbocyanine (Dil-C_{18}) was purchased from Invitrogen. Dulbecco's Modified Eagle Medium (DMEM) and foetal bovine serum (FBS) were obtained from Gibco. FITC-labelled anti-F4/80 monoclonal antibody (clone BM8) was obtained from Biolegend. Cholesterol, [1,2-3H(N)]-, 1 mCi (37 MBq) and Ultima Gold were obtained from Perkin Elmer. Trehalose and hydrogen peroxide 30% v/w were purchased from Acros Organics. Penicillin-streptomycin, L-glutamine, cholesterol (Chol) and pontamine blue were purchased from Sigma.

Formulation of liposomes by microfluidics

Liposomes were prepared in the Nanoassemblr Platform (Precision Nanosystems Inc.) in a Y-shaped staggered herringbone micromixer of 300 µm width and 130 µm height. Briefly, DOPE:DOTAP and DOPE:DDA lipid mixtures were prepared in methanol at 1:1 molar ratio. Then, the lipids and an aqueous phase (TRIS buffer pH 7.4) were injected simultaneously in the micromixer. All formulations were prepared at 4 mg/mL initial lipid concentration, 1:1 aqueous:organic flow rate ratio (FRR) and 15 mL/min total flow rate (TFR). The TRIS buffer concentration was varied from 10 to 1000 mM to prepare size-tuneable liposomes. All newly formed liposomes (1mL) were then subjected to buffer exchange via dialysis against 10 mM TRIS pH 7.4 for 1 hour under magnetic stirring to ensure all liposomes were in a 10 mM TRIS pH 7.4 (Figure 1). For *in vitro* cellular uptake experiments, liposomes were formulated incorporating the lipophilic fluorescent dye Dil-C_{18} (0.2 mol %) within the bilayer. Any non-incorporated free Dil-C_{18} dye (MW = 933 Da) was removed via dialysis (cut off = 14,000 Da).

Liposome characterization

All liposome formulations were characterized, after dialysis, in terms of hydrodynamic size (Z-average), polydispersity index (PDI) and surface charge (zeta-potential) by dynamic light scattering (DLS) in a Zetasizer Nano ZS (Malvern, UK) at a liposome concentration of 0.1 mg/mL in 10 mM TRIS pH 7.4 at 25 °C.

Cryo-TEM

Liposome samples (3 µL) were deposited on a pre-cleaned lacey carbon-coated grid and flashed frozen by plunging into liquid ethane cooled by liquid nitrogen. Samples were then observed in a cryo-holder

in electron microscope Tecnai 12 G2 (FEI, Eindhoven) at liquid nitrogen temperature and 80 KV with magnifications ranging from 40,000X to 135,000X.

Bone marrow-derived macrophages (BMDM)

Bone marrow cells, obtained from femur and tibiae of 6-8-week-old male BALB/c mice, were incubated in petri dishes in macrophage medium: DMEM supplemented with 20% heat-inactivated foetal bovine serum (HI-FBS), 0.1 mg/mL penicillin-streptomycin, 4 mM L-glutamine and 20% L-Cell conditioned medium (supernatant obtained from confluent L929 fibroblast cell line) at 37 °C, 95% humidity and 5% CO_2 in a cell incubator (Panasonic). A total of 4 petri dishes (10 mL) were obtained per mice. At day 2, fresh macrophage medium (10 mL) was added to each petri dish. At day 7, 15 mL of media were removed from each petri dish and replaced with 15 mL of fresh macrophage medium. At day 10, cells were scraped, washed and cultured in 24-well plates in DMEM supplemented with 10% HI-FBS, 0.1 mg/mL penicillin-streptomycin and 4 mM L-glutamine (complete DMEM, or cDMEM) at $2{\cdot}10^5$ cells/well and were allowed to adhere for 24 hours at 37 °C and 5% CO_2. The percentage of BMDM was determined as percentage of F4/80$^+$ cells. F4/80 is a membrane glycoprotein that has been widely used as a specific cell marker for murine macrophages [33]. Briefly, a total of $2{\cdot}10^5$ cells were incubated with a FITC-labelled anti-F4/80$^+$ monoclonal antibody (1/200 dilution) in FACS buffer (PBS supplemented with 5% FBS) for 30 min at 4 °C, washed twice and analysed by flow cytometry (FACSCanto, BD Biosciences).

***In vitro* liposome uptake by BMDM**

BMDM were incubated with Dil-C_{18}-labeled cationic liposomes (10 µg/mL) for 1, 4 and 24 hours at 37 °C. They were then scraped and washed twice. Subsequently, liposome-cell interactions were quantified by flow cytometry (FACSCanto, BD Biosciences). The lipophilic dye Dil-C_{18} can be only incorporated within the lipid bilayer and thus its concentration is constant for unilamellar liposomes regardless of liposome size. Therefore, liposome fluorescence can be expressed as:

$$\text{eq (1) Liposome fluorescence} \equiv \mathrm{F_m} \cdot [\mathrm{Dil-C_{18}}] \cdot \frac{4}{3}\Pi[\mathrm{r^3} - (\mathrm{r}-5)^3]$$

Where F_m is the fluorescence of Dil-C_{18}, r is the liposome radius (estimated by DLS) and 5 is the lipid bilayer thickness (in nm) estimated from cryo-TEM images of unilamellar 40 nm DOPE:DOTAP liposomes. The mean fluorescence intensity measured by flow cytometry is equivalent to the amount of fluorescent dye taken up by BMDM, which is directly proportional to the product of the number of

liposomes by liposome fluorescence. Hence, the relative number of liposomes (N_r), liposome surface (SA_r) area and liposome internal volume (V_r) can be deducted:

$$\text{eq (2) Relative number of liposomes } (N_r) \equiv \frac{\text{Mean Fluorescence Intensity}}{\frac{4}{3}\Pi[r^3 - (r-5)^3]}$$

$$\text{eq (3) Relative liposome surface area } (SA_r) \equiv N_r \cdot 4\Pi r^2$$

$$\text{eq (4) Relative liposome internal volume } (V_r) \equiv N_r \cdot \frac{4}{3}\Pi(r-5)^3$$

Although no absolute values are obtained with these equations, direct comparisons can be made among liposomes of different size.

Biodistribution studies

All *in vivo* studies were conducted under the regulations of the Directive 2010/63/EU. All protocols were subjected to ethical review and were carried out in a designated establishment. The *in vivo* biodistribution of cationic liposomes was studied in 4-5-week-old female CD1 mice (20 – 25 g). In order to track their movement, liposomes were radiolabelled with ^{3}H-cholesterol. In brief, ^{3}H-cholesterol was incorporated to the lipid mixture, and liposomes were formulated by microfluidics and dialyzed against 10 mM TRIS pH 7.4. Finally, trehalose was added to a final concentration of 10% w/v to maintain isotonicity upon injection. Each dose (50 µL) contained 50 µg of DOPE, 50 µg of cationic lipid (DOTAP or DDA) and 25 ng of ^{3}H-cholesterol (200 KBq/dose). The concentration of cholesterol was low enough not to change the size of liposomes. 3 – 4 days before injection, mice were injected with 200 µL of Chicago Blue (0.5 % w/v) subcutaneously into the neck scruff as a marker for lymph nodes. Formulations were injected (50 µL) intramuscularly in the right quadriceps muscle. Mice were terminated at relevant time points (6, 24, 48, 72 and 96 h) post injection (p.i), and tissue from the injection site and draining lymph nodes (popliteal lymph node – PLN, inguinal lymph node – ILN) on the side of the injection site were collected for analysis. Briefly, samples were solubilized completely in 10 M NaOH (2 mL) at 60 °C overnight and subsequently bleached with 30% w/v hydrogen peroxide (200 µL) for 2 h at 60 °C. Then, 10 mL of Ultima Gold Scintillation cocktail were added. Radiation was quantified in a Liquid Scintillation Analyser Tri-Carb 2810 TR (Perkin Elmer). The percentage of injected dose was calculated with respect to the original dose as follows:

$$\%\text{ of injected dose} = \frac{\text{counts (cpm) in organ}}{\text{counts (cpm) in original dose}} \text{ x } 100$$

Statistical Analysis

Statistical analysis of cellular uptake experiments was performed on the mean of at three replicates by one-way analysis of variance (ANOVA) followed Tukey's honest significance test in GraphPad Prism version 7 (GraphPad Software Inc., La Jolla, CA). To compare the biodistribution of the liposomes, the area under the curve for biodistribution was calculated for each mouse, and the mean calculated. These were then compared using the t-test (Excel) to consider significance ($p<0.05$).

Results

Formulation of size-tuneable liposomes by microfluidics

Previous studies have suggested that salt concentration can control liposome formation. For example, Meyuhas et al. reported that lipid vesicles composed of phosphatidylcholine (PC) and sodium cholate, prepared in 10 mM TRIS (pH 7.4), increased in size from 40 to 100 nm by adding increasing NaCl concentration up to 500 mM [34]. We explored this concept in the context of microfluidic production of liposome and buffer ionic strength (TRIS buffer) where liposomes are prepared with varying buffer concentrations and then the buffer concentration re-set to 10 mM TRIS (Figure 1). Results shown in Figure 2 demonstrate that cationic liposome size could be controlled by varying the electrolyte concentration used in the initial preparation, whilst neutral formulations were not sensitive to changes in the electrolyte concentration range considered. Neutral liposomes, composed of DSPC:Chol, remained at approximately 80 nm in size over TRIS buffer concentrations of 0 to 1000 mM (Figure 2A). In contrast, cationic liposomes composed of DOPE:DOTAP increased in size stepwise from 40 to over 600 nm over the same TRIS concentration range (Figure 2A). This increase in size with increasing buffer concentration was even more notable with DOPE:DDA, with 350 mM TRIS being sufficient to produce vesicles of 600 nm in size (Figure 1A). Interestingly, DOPE:DDA liposomes did not form at higher ionic strengths, and resulted in macroscopic lipid aggregation; probably due to an excessive increase of P_C. Notably, all formulations exhibited low PDI (0.05 – 0.25) regardless of liposome size (Figure 2B). Furthermore, the cationic liposomes exhibited highly positive zeta-potential (40 – 60 mV) and DSPC:Chol liposomes slightly negative across the buffer concentration range tested (Figure 2C). All three formulations exhibited narrow unimodal size distribution irrespective of the size and buffer concentration they were initially prepared in (Figures 2D to F) and the effect of initial buffer concentration on liposome size could also be easily observed visually with both the DOTAP (Figure 2D) and DDA (Figure 2E) showing notable increases in turbidity, whilst DSPC:Chol remained the same (Figure 2F). Cryo-TEM characterization of small and large liposomes further confirmed that this approach allows to increase P_c enough to obtain large liposomes but not enough to induce formation of other lipid aggregates. Indeed, both small (Figure 3A and B) and large DOPE:DOTAP liposomes (Figure 3C and D) were uni/oligolamellar and had a size and size distribution that matched with DLS measurements (Figure 3E and F).

To investigate to what extent the cationic lipid was responsible of increased liposome size, DSPC:Chol liposomes were formulated with increasing molar percentages of DOTAP (0, 5, 13 and 23%) (Figure 4) and DDA (13 and 23%). With the DOTAP formulations, the impact of buffer concentration on particle size increased with cationic lipid content (Figure 4); with formulations containing low DOTAP levels increasing up to 112 nm whilst formulations containing 5 and 13% DOTAP increasing to 140 nm and 175 nm respectively. However, increasing the molar percentage of DOTAP to 23% did not result in larger liposomes (Figure 4A). In general, all PDI values were low (<0.2) with the exception of the 23% DOTAP formulation at 1000 mM TRIS, where the PDI rose to 0.3 (Figure 4B). In terms of their zeta-potential, DSPC:Chol liposomes were slightly negative (approximately -15 mV) and increasing the cationic lipid content increased the zeta potential as would be expected (Figure 4C). When considering the addition of DDA (13% and 23%) to the DSPC:Chol formulations, liposomes did not change in size at increasing concentrations of TRIS buffer and remained at 120 – 140 nm, PDI < 0.2 (data not shown).

To consider if this size-controlling effect was achievable with other buffers, the effect of ionic strength was also investigated on citrate buffer pH 6. Citrate buffer is often used in the preparation of RNA lipid nanoparticles (LNP) containing ionizable/cationic lipids. We first attempted to formulate DOPE:DOTAP and DOPE:DDA liposomes in citrate buffer, but all formulations aggregated regardless of citrate concentration. Therefore only DSPC:Chol and DSPC:Chol:DOTAP (5% DOTAP) formulations were tested. Interestingly, when DSPC:Chol liposomes were formulated in citrate buffer pH 6.0, a small but significant ($p < 0.05$) increase in vesicle size from 80 to 120 nm was noted (Figure 4D), while it did not increase when formulated at same concentrations of TRIS pH 7.4 (Figure 2A). The 9% DOTAP liposome formulation also displayed a trend of increasing size (from 98 to 166 nm) with increasing citrate buffer concentration, and only 400 mM was required to obtain liposomes of same size achievable with 1000 mM TRIS buffer (Figure 4D). As with the TRIS formulations, the PDI of all formulations tested remained low (<0.25) (Figure 4E).

The effect of vesicle size on liposome-cell interactions

The effect of vesicle size on the liposome-cell interactions was investigated in BMBM with DOPE:DOTAP and DOPE:DDA liposomes. Small (40 nm) and large (>500 nm) liposomes were prepared by microfluidics by changing buffer ionic strength. Small DOPE:DOTAP and DOPE:DDA liposomes had a size of 40 – 45 nm, while their larger counterparts were approximately 750 and 500 nm respectively. All formulations had a PDI between 0.15 and 0.25 and a highly positive zeta-potential (40 – 60 mV) (table 1).

The percentage of $F4/80^{+}$ cells, relative to bone marrow-derived macrophages (BMDM) after bone marrow cell differentiation was at least 95% as determined by flow cytometry (data not shown). The

in vitro experiments were carried out at liposome concentrations of 10 µg/mL. The same concentration of 40 nm DOPE:DOTAP and DOPE:DDA liposomes was shown to be non-toxic after 24 hours (>90% survival, data not shown). We first investigated the interactions of cationic (40 nm DOPE:DOTAP) liposomes with BMDM at 4 °C, temperature at which endocytosis is inhibited. At such temperature, the percentage of Dil-C_{18}^{+} cells was 11% after 1 hour and did not increase over time. Similarly, the mean fluorescence intensity (MFI), which is proportional to the amount of cell-associated dye (surface-associated or internalized) was <1000 in the same time frame (Figure S1). These results suggest that, at 4 °C, cationic liposomes partially interact with BMDM with no further internalization.

In contrast, at 37 °C, all liposome formulations rapidly interacted with BMDM irrespective of lipid choice and liposome size (Figure 5), with approximately 50, 80 and 100% of Dil-C_{18}^{+}(i.e. liposome^{+}) cells after 1, 4, and 24 hours (Figure 5A). The MFI was approximately 1200 after 1 hour and and increased over 6000 after 24 hours for all formulations in a similar manner (Figure 5B). Considering the results shown in Figures S1 and 5, it seems that, after 1 hour, a significant percentage of cationic liposomes is surface-associated, while the real liposome internalization occurs at some point between 1 and 4 hours. Indeed, after 4 and 24 hours, both the percentage of Dil-C_{18}^{+} cells and the MFI at 37 °C were significantly higher than at 4 °C.

BMDM uptake was also analysed in terms of relative number of liposomes (N_r), relative liposome surface area (SA_r) and relative liposome internal volume (V_r). While SA_r did not vary with size (Figure 5C), the effect of liposome size on BMDM uptake became more evident when looking at N_r and V_r. The N_r of small DOPE:DOTAP and DOPE:DDA liposomes taken up by BMDM was 400 – 500 and 200 – 300 fold higher than their larger counterparts (Figure. 5D). However, the situation is the opposite for V_r. Indeed, the V_r taken up by BMDM was 12 – 18 and 20 – 26 fold higher when larger DOPE:DOTAP and DOPE:DDA liposomes were used (Figure. 5E) thereby showing the potential advantage of large liposomes over small ones to deliver hydrophilic drugs.

The effect of vesicle size on biodistribution

To consider if the size of these vesicles had an effect on their biodistribution *in vivo*, small (40 nm) and large (500 – 750 nm) DOPE:DOTAP and DOPE:DDA liposomes were injected intramuscularly and their distribution monitored over 96 h. Both liposome formulations were retained at the injection site with low levels of liposomes draining to the local lymph nodes (Figure 6). To compare the distributions, the area under the curve (AUC) was calculated and the mean AUCs for each group compared.

With both formulations, the small cationic liposomes have trend to distribute from the injection site more rapidly than the similar larger counterpart. For example, with the DDA formulation, 92 % of large

DOPE:DDA large liposomes retained at the injection site after 24 h compared to 68 % with the small DOPE:DDA formulation. This difference continues to 96 h with 54% and 36 % of the large and small vesicles respectively remaining at the injection site (Figure 6D). These differences were confirmed to be significant ($p<0.05$) when comparing the AUC for both the cationic lipids, with the smaller liposome formulations having a significantly lower AUC than their larger rmulation counterparts (3847 vs 5462 %Dose.h for small and large DOTAP liposomes and 4689 vs 6402 %Dose.h for small and large DDA). Similarly, when comparing the distribution of these liposomes to the local draining lymph nodes, we see the smaller liposomes showing an increased accumulation at both the PLN (Figure 6B and E) and ILN (Figure 6C and F) with significantly higher ($p<0.05$) AUC for smaller liposomes (irrespective of the lipid choice) at both lymph nodes. However, across all formulations, only low levels (<0.6%) of the dose injected was measured at both the popliteal and inguinal lymph nodes irrespective of liposome composition and size.

Discussion

Microfluidics provides a unique tool to formulate liposomes with consistent size and size distribution compared to conventional methods such as extrusion or probe sonication. Although liposome size can be controlled via adjustments of microfluidic operating parameters such as flow rate ratio, total flow rate and lipid concentration, liposomes can only be prepared within a limited size range (approximately from 25 to 300 nm [6, 9, 11, 12, 26, 35, 36]) depending on lipid composition and micromixer design. A microfluidic method from producing larger but still monodisperse and unilamellar liposomes would be therefore highly advantageous.

Previous studies have shown that electrolyte concentration can control the formation of lipid self-assemblies. Lipid vesicles composed of PC and sodium cholate increased in size from 40 to 100 nm by increasing NaCl concentration from 0 to 500 mM [34]. Similarly, Edwards and co-workers prepared vesicles composed of PC and cetyltrimethylammonium chloride and observed a vesicle-to-micelle transition and an increase in vesicle size over time in presence of 100 mM NaCl which did not occur in absence of salt [37]. Electrolytes (NaCl, Ca^{2+}) were also reported to induce lamellar-to-cubic phase transitions in lipid membranes consisting of monoolein and other lipid, such as dioleoylphosphatidylglycerol [38], dioleoylphosphatidylserine [39, 40], and also in pre-formed liposomes composed of phytantriol and DDA [41]. Indeed, electrolytes reduce repulsion among lipid head groups and consequently increase the packing parameter of lipids (P_c), thereby reducing the curvature of the lipid self-assemblies. At sufficiently high electrostatic repulsion, negative curvature values are obtained and, therefore, non-liposomal self-assemblies (e.g. inverted micelles or cubosomes) are expected. A modest electrostatic repulsion, however, can potentially reduce the

curvature of the lipid bilayer enough to increase liposome size but not enough to promote formation of non-liposomal structures.

Herein, we exploited this concept on the microfluidic formation of cationic liposomes (Figure 1), and demonstrated that the size of cationic DOPE:DOTAP and DOPE:DDA liposomes increased from 40 up to >500 nm by increasing the concentration of the aqueous phase (TRIS pH 7.4) in the range of 10 to 1000 mM, with DOPE:DDA liposomes requiring lower buffer concentrations to achieve the same size than DOPE:DOTAP liposomes. Importantly, cationic liposomes exhibited low PDI, narrow and unimodal size distribution and consistent zeta-potential; whilst the size of zwitterionic DSPC:Chol liposomes (80 nm) was not influenced by TRIS concentration (Figure 2). Cryo-TEM analysis confirmed the ability to produce both SUV and LUV (Figure 3). Furthermore, buffer concentration-dependent liposome size was influenced by both percentage of cationic lipid within the formulation and the type of buffer, as observed with DSPC:Chol:DOTAP liposomes (0, 5, 13 and 23% DOTAP) (Figure 4). Considering the results shown in Figure 2, one would expect that the substitution of DOTAP for DDA in the latter formulation would allow obtaining larger liposomes with relatively lower buffer concentrations. DSPC:Chol:DDA (13 and 23% DDA) liposomes (120 – 140 nm, PDI < 0.2) did not increase in the range of 10 to 1000 mM TRIS. Both shape and size of lipid aggregates can be predicted by the packing parameter. For lipid mixtures, a mean packing parameter between those of the individual lipids may be considered if only if the different molecules mix ideally and do not phase-separate, such that vesicle size can be tuned by adding a lipid with a higher (or lower) packing parameter [16, 42]. From this point of view, the combination of DDA with DSPC and Chol may result in an asymmetrical distribution of lipids throughout the lipid bilayer thereby inhibiting the effect of ionic strength. These results show that different buffer-dependent liposome sizes are expected for specific combinations of cationic and structural lipids. Both buffer concentration and type of buffer are hence important parameters to tune liposome size by microfluidics. We took advantage of this method to produce cationic unilamellar liposomes of two different size ranges to investigate the effect of liposome size *in vitro* and *in vivo*. For doing so, we made use of small (40 nm) and large (>500 nm) DOPE:DOTAP and DOPE:DDA liposomes (table 1).

In vitro, at 37 °C, cationic liposomes rapidly interacted with murine bone marrow-derived macrophages (BMDM), with approximately 50% Dil-C_{18}^{+} (i.e. liposome^{+}) cells and a MFI of 1200 after 1 hour Both the percentage of Dil-C_{18}^{+} cells and the mean fluorescence intensity (MFI) increased in a similar manner over time (100% and over 6000 respectively) regardless of liposome composition and size (Figure 5 A and B). In contrast, at 4 °C, temperature at which endocytosis is inhibited, interaction of cationic (40 nm DOPE:DOTAP) liposomes was restrained, with only 11% of positive cells and a MFI <1000 respectively regardless of the incubation time (Figure S1), thus suggesting that, at 4 °C, cationic

liposomes interact with BMDM with no further internalization. Similar values of MFI at 4 and 37 °C suggest that, after 1 hour, of cationic liposomes could be surface-associated rather than internalized. However, the contribution of surface-associated liposomes (given at 4 °C) could be considered negligible at 4 and 24 hours and therefore would be related to cellular uptake rather than a combination of surface-associated and internalized liposomes. Furthermore, these findings are opposite to previous reports, where cellular uptake was reported to increase with increasing liposome size [43-46]. It should be considered, however, that in these studies liposomes were prepared by lipid film hydration followed by extrusion and therefore the degree of lamellarity was not controlled. Furthermore, in some cases liposome uptake was quantified by radio-counting a radiolabelled nonexchangeable lipid and hence the cellular uptake of large liposomes may have been overestimated because of liposome lamellarity. Indeed, the amount of 1000 nm liposomes taken up by peritoneal macrophages *in vitro* (ng lipid per µg protein) was shown to be 2-fold lower compared to MLV of comparable size [46]. However, within our studies, differential uptake of small and large cationic liposomes by BMDM was more evident when analysed in terms of relative number of liposomes (N_r), relative liposome surface area (SA_r) and relative liposome internal volume (V_r). SA_r did not vary with size (Figure 5C), while N_r and V_r decreased (>200-fold) and increased (>10 fold) respectively by increasing liposome size from 40 to above 500 nm (Figure 5D and E). A microfluidic-based approach was also used elsewhere to show that the cellular uptake of uniform (PDI < 0.05) unilamellar liposomes, ranging from 40 to 275 nm, improved (in terms of number of internalized liposomes) with reducing liposome size in the Caco-2 cell line [26]. Similar results were observed on mouse peritoneal macrophages by Hsu and Juliano [46] and Schwendener et al. [47]. In the first study, uptake of small unilamellar liposomes (35 nm) was 100-fold higher, in terms of liposome number, compared to 1000 nm liposomes, but 100-fold lower when represented as internal volume. In the second study, reducing liposome size from 180 to 25 nm resulted in 100-fold increase of cell-associated vesicles but 10-fold reduction in trapped volume.

Different pharmacokinetic profiles were also observed *in vivo* for small (40 nm) and large (>500 nm) cationic liposomes upon intramuscular injection, with large liposomes showing longer retention at the injection site but limited drainage to the local lymph nodes compared to small liposomes (Figure 6). Studies conducted with the vaccine adjuvant CAF01, composed of DDA and trehalose 6,6'-dibehenate (TDB), and its associated antigen (Ag85B-ESAT-6) revealed that cationic liposomes from 200 to >2000 nm exhibited similar clearance rates from the injection site upon intramuscular injection [27, 28]. Furthermore, to promote clearance from the injection site of this formulation, both size reduction and PEGylation was employed [28] . However, it has previously been difficult to achieve the production of cationic liposomes in the size ranges achieved within this current manuscript and our results suggest

that by formulating these highly cationic liposomes down to 40 nm allows us to modify their pharmacokinetic profile after intramuscular injection. Indeed, in recent studies looking at the distribution of cationic chitosan nanocapsules after sub-cutaneous administration, 100 nm particles drained more rapidly to the lymph nodes compared to those of 200 nm and this size reduction also improved interaction with both migratory and resident antigen presenting cells in the lymph nodes, suggesting a combination of free- and cell-mediated transport to the lymph nodes [48]. This could explain why similar pharmacokinetic profiles were observed for CAF01 formulated at different, since none of the formulations were below 100 nm. Indeed, depletion of dendritic cells *in vivo* completely abolished trafficking of 500 nm polystyrene particles to the LN but not affected drainage of 20 nm particles [49]. Therefore, in our studies where we have been able to prepare cationic liposomes below 50 nm, we are able to modify the biodistribution potentially through a combination of free- and cell-mediated transport to the lymph nodes.

C**onclusions**

In the current study, we have demonstrated a new microfluidic process to produce monodisperse size-tuneable cationic large unilamellar liposomes of up to 750 nm (depending on the lipid composition). We also demonstrate the size-dependent *in vitro* cellular uptake of cationic liposomes in murine bone marrow-derived macrophages (BMDM) in terms of relative liposome number, liposome surface area, and liposome internal volume. Moreover, we demonstrate we are able to modify the clearance rates of these liposomes from the injection site and increase accumulation to the draining lymphatics. This is despite their highly cationic nature and propensity to aggregate in the presence of interstitial proteins and their movement to the local lymphatics may result from both free- and cellular mediated transport.

Acknowledgements.

This work was funded by the European Commission Project *Leveraging Pharmaceutical Sciences and Structural Biology Training to Develop 21st Century Vaccines* (H2020-MSCA-ITN-2015 grant agreement 675370).

Supporting information Available

Data presented in this publication can be found at https://doi.org/10.15129/c8a0e9ff-de6d-4060-886e-a3196279f084.

460 **References**

461 [1] A.D. Bangham, M.M. Standish, J.C. Watkins, Diffusion of univalent ions across the lamellae of
462 swollen phospholipids, Journal of Molecular Biology, 13 (1965) 238-IN227.
463 [2] D. Christensen, K.S. Korsholm, I. Rosenkrands, T. Lindenstrøm, P. Andersen, E.M. Agger, Cationic
464 liposomes as vaccine adjuvants, Expert review of vaccines, 6 (2007) 785-796.
465 [3] C.R. Safinya, K.K. Ewert, R.N. Majzoub, C. Leal, Cationic liposome-nucleic acid complexes for gene
466 delivery and gene silencing, New journal of chemistry = Nouveau journal de chimie, 38 (2014) 5164-
467 5172.
468 [4] P.C. Englezou, C. Sapet, T. Démoulins, P. Milona, T. Ebensen, K. Schulze, C.-A. Guzman, F. Poulhes,
469 O. Zelphati, N. Ruggli, K.C. McCullough, Self-Amplifying Replicon RNA Delivery to Dendritic Cells by
470 Cationic Lipids, Molecular Therapy - Nucleic Acids, 12 (2018) 118-134.
471 [5] M. Pons, M. Foradada, J. Estelrich, Liposomes obtained by the ethanol injection method,
472 International journal of pharmaceutics, 95 (1993) 51-56.
473 [6] A. Jahn, W.N. Vreeland, M. Gaitan, L.E. Locascio, Controlled vesicle self-assembly in microfluidic
474 channels with hydrodynamic focusing, Journal of the American Chemical Society, 126 (2004) 2674-
475 2675.
476 [7] H.-H. Jeong, D. Issadore, D. Lee, Recent developments in scale-up of microfluidic emulsion
477 generation via parallelization, Korean Journal of Chemical Engineering, 33 (2016) 1757-1766.
478 [8] S. Joshi, M.T. Hussain, C.B. Roces, G. Anderluzzi, E. Kastner, S. Salmaso, D.J. Kirby, Y. Perrie,
479 Microfluidics based manufacture of liposomes simultaneously entrapping hydrophilic and lipophilic
480 drugs, International journal of pharmaceutics, 514 (2016) 160-168.
481 [9] A. Jahn, S.M. Stavis, J.S. Hong, W.N. Vreeland, D.L. DeVoe, M. Gaitan, Microfluidic mixing and the
482 formation of nanoscale lipid vesicles, ACS nano, 4 (2010) 2077-2087.
483 [10] N. Forbes, M.T. Hussain, M.L. Briuglia, D.P. Edwards, J.H.t. Horst, N. Szita, Y. Perrie, Rapid and
484 scale-independent microfluidic manufacture of liposomes entrapping protein incorporating in-line
485 purification and at-line size monitoring, International journal of pharmaceutics, 556 (2019) 68-81.
486 [11] A. Jahn, W.N. Vreeland, D.L. DeVoe, L.E. Locascio, M. Gaitan, Microfluidic directed formation of
487 liposomes of controlled size, Langmuir, 23 (2007) 6289-6293.
488 [12] D. Carugo, E. Bottaro, J. Owen, E. Stride, C. Nastruzzi, Liposome production by microfluidics:
489 potential and limiting factors, 6 (2016) 25876.
490 [13] M. Guimaraes Sa Correia, M.L. Briuglia, F. Niosi, D.A. Lamprou, Microfluidic manufacturing of
491 phospholipid nanoparticles: Stability, encapsulation efficacy, and drug release, International journal
492 of pharmaceutics, 516 (2017) 91-99.
493 [14] E. Kastner, V. Verma, D. Lowry, Y. Perrie, Microfluidic-controlled manufacture of liposomes for
494 the solubilisation of a poorly water soluble drug, International journal of pharmaceutics, 485 (2015)
495 122-130.
496 [15] J.N. Israelachvili, S. Marcelja, R.G. Horn, Physical principles of membrane organization, Quarterly
497 reviews of biophysics, 13 (1980) 121-200.
498 [16] J.N. Israelachvili, Intramolecular and Surface Forces, Academic Press, New York, 1992.
499 [17] M. Henriksen-Lacey, D. Christensen, V.W. Bramwell, T. Lindenstrom, E.M. Agger, P. Andersen, Y.
500 Perrie, Liposomal cationic charge and antigen adsorption are important properties for the efficient
501 deposition of antigen at the injection site and ability of the vaccine to induce a CMI response, Journal
502 of controlled release : official journal of the Controlled Release Society, 145 (2010) 102-108.
503 [18] T.M. Allen, J.M. Everest, Effect of liposome size and drug release properties on pharmacokinetics
504 of encapsulated drug in rats, The Journal of pharmacology and experimental therapeutics, 226 (1983)
505 539-544.
506 [19] J.M. Brewer, L. Tetley, J. Richmond, F.Y. Liew, J. Alexander, Lipid vesicle size determines the Th1
507 or Th2 response to entrapped antigen, Journal of immunology (Baltimore, Md. : 1950), 161 (1998)
508 4000-4007.

[20] R. Kaur, V.W. Bramwell, D.J. Kirby, Y. Perrie, Pegylation of DDA:TDB liposomal adjuvants reduces the vaccine depot effect and alters the Th1/Th2 immune responses, Journal of controlled release : official journal of the Controlled Release Society, 158 (2012) 72-77.
[21] G.V. Betageri, D.L. Parsons, Drug encapsulation and release from multilamellar and unilamellar liposomes, International journal of pharmaceutics, 81 (1992) 235-241.
[22] H. Epstein-Barash, D. Gutman, E. Markovsky, G. Mishan-Eisenberg, N. Koroukhov, J. Szebeni, G. Golomb, Physicochemical parameters affecting liposomal bisphosphonates bioactivity for restenosis therapy: internalization, cell inhibition, activation of cytokines and complement, and mechanism of cell death, Journal of controlled release : official journal of the Controlled Release Society, 146 (2010) 182-195.
[23] S.A. Johnstone, D. Masin, L. Mayer, M.B. Bally, Surface-associated serum proteins inhibit the uptake of phosphatidylserine and poly(ethylene glycol) liposomes by mouse macrophages, Biochimica et Biophysica Acta (BBA) - Biomembranes, 1513 (2001) 25-37.
[24] S. Takano, Y. Aramaki, S. Tsuchiya, Physicochemical Properties of Liposomes Affecting Apoptosis Induced by Cationic Liposomes in Macrophages, Pharmaceutical research, 20 (2003) 962-968.
[25] S. Dabbas, R.R. Kaushik, S. Dandamudi, G.M. Kuesters, R.B. Campbell, Importance of the Liposomal Cationic Lipid Content and Type in Tumor Vascular Targeting: Physicochemical Characterization and In Vitro Studies Using Human Primary and Transformed Endothelial Cells, Endothelium, 15 (2008) 189-201.
[26] A.U. Andar, R.R. Hood, W.N. Vreeland, D.L. Devoe, P.W. Swaan, Microfluidic preparation of liposomes to determine particle size influence on cellular uptake mechanisms, Pharmaceutical research, 31 (2014) 401-413.
[27] M. Henriksen-Lacey, A. Devitt, Y. Perrie, The vesicle size of DDA:TDB liposomal adjuvants plays a role in the cell-mediated immune response but has no significant effect on antibody production, Journal of controlled release : official journal of the Controlled Release Society, 154 (2011) 131-137.
[28] R. Kaur, V.W. Bramwell, D.J. Kirby, Y. Perrie, Manipulation of the surface pegylation in combination with reduced vesicle size of cationic liposomal adjuvants modifies their clearance kinetics from the injection site, and the rate and type of T cell response, Journal of controlled release : official journal of the Controlled Release Society, 164 (2012) 331-337.
[29] M.G. Carstens, M.G.M. Camps, M. Henriksen-Lacey, K. Franken, T.H.M. Ottenhoff, Y. Perrie, J.A. Bouwstra, F. Ossendorp, W. Jiskoot, Effect of vesicle size on tissue localization and immunogenicity of liposomal DNA vaccines, Vaccine, 29 (2011) 4761-4770.
[30] S. Khadke, C.B. Roces, A. Cameron, A. Devitt, Y. Perrie, Formulation and manufacturing of lymphatic targeting liposomes using microfluidics, (Submitted).
[31] J.M. Brewer, K.G.J. Pollock, L. Tetley, D.G. Russell, Vesicle Size Influences the Trafficking, Processing, and Presentation of Antigens in Lipid Vesicles, The Journal of Immunology, 173 (2004) 6143.
[32] A. Badiee, A. Khamesipour, A. Samiei, D. Soroush, V.H. Shargh, M.T. Kheiri, F. Barkhordari, W. Robert Mc Master, F. Mahboudi, M.R. Jaafari, The role of liposome size on the type of immune response induced in BALB/c mice against leishmaniasis: rgp63 as a model antigen, Experimental parasitology, 132 (2012) 403-409.
[33] J.M. Austyn, S. Gordon, F4/80, a monoclonal antibody directed specifically against the mouse macrophage, European journal of immunology, 11 (1981) 805-815.
[34] D. Meyuhas, A. Bor, I. Pinchuk, A. Kaplun, Y. Talmon, M.M. Kozlov, D. Lichtenberg, Effect of Ionic Strength on the Self-Assembly in Mixtures of Phosphatidylcholine and Sodium Cholate, Journal of Colloid and Interface Science, 188 (1997) 351-362.
[35] E. Kastner, R. Kaur, D. Lowry, B. Moghaddam, A. Wilkinson, Y. Perrie, High-throughput manufacturing of size-tuned liposomes by a new microfluidics method using enhanced statistical tools for characterization, International journal of pharmaceutics, 477 (2014) 361-368.
[36] R.R. Hood, D.L. DeVoe, High-Throughput Continuous Flow Production of Nanoscale Liposomes by Microfluidic Vertical Flow Focusing, Small, 11 (2015) 5790-5799.

[37] K. Edwards, J. Gustafsson, M. Almgren, G. Karlsson, Solubilization of Lecithin Vesicles by a Cationic Surfactant: Intermediate Structures in the Vesicle-Micelle Transition Observed by Cryo-Transmission Electron Microscopy, Journal of Colloid and Interface Science, 161 (1993) 299-309.
[38] T.S. Awad, Y. Okamoto, S.M. Masum, M. Yamazaki, Formation of Cubic Phases from Large Unilamellar Vesicles of Dioleoylphosphatidylglycerol/Monoolein Membranes Induced by Low Concentrations of Ca2+, Langmuir, 21 (2005) 11556-11561.
[39] T. Oka, M. Hasan, M.Z. Islam, M. Moniruzzaman, M. Yamazaki, Low-pH-Induced Lamellar to Bicontinuous Primitive Cubic Phase Transition in Dioleoylphosphatidylserine/Monoolein Membranes, Langmuir, 33 (2017) 12487-12496.
[40] M.M. Alam, T. Oka, N. Ohta, M. Yamazaki, Kinetics of low pH-induced lamellar to bicontinuous cubic phase transition in dioleoylphosphatidylserine/monoolein, The Journal of Chemical Physics, 134 (2011) 145102.
[41] B.W. Muir, G. Zhen, P. Gunatillake, P.G. Hartley, Salt Induced Lamellar to Bicontinuous Cubic Phase Transitions in Cationic Nanoparticles, The Journal of Physical Chemistry B, 116 (2012) 3551-3556.
[42] S. Carnie, J.N. Israelachvili, B.A. Pailthorpe, Lipid packing and transbilayer asymmetries of mixed lipid vesicles, Biochimica et Biophysica Acta (BBA) - Biomembranes, 554 (1979) 340-357.
[43] S. Chono, Y. Tauchi, K. Morimoto, Influence of particle size on the distributions of liposomes to atherosclerotic lesions in mice, Drug development and industrial pharmacy, 32 (2006) 125-135.
[44] S. Chono, T. Tanino, T. Seki, K. Morimoto, Uptake characteristics of liposomes by rat alveolar macrophages: influence of particle size and surface mannose modification, Journal of Pharmacy and Pharmacology, 59 (2010) 75-80.
[45] S. Chono, T. Tanino, T. Seki, K. Morimoto, Influence of particle size on drug delivery to rat alveolar macrophages following pulmonary administration of ciprofloxacin incorporated into liposomes, Journal of drug targeting, 14 (2006) 557-566.
[46] M.J. Hsu, R.L. Juliano, Interactions of liposomes with the reticuloendothelial system: II. Nonspecific and receptor-mediated uptake of liposomes by mouse peritoneal macrophages, Biochimica et Biophysica Acta (BBA) - Molecular Cell Research, 720 (1982) 411-419.
[47] R.A. Schwendener, P.A. Lagocki, Y.E. Rahman, The effects of charge and size on the interaction of unilamellar liposomes with macrophages, Biochimica et biophysica acta, 772 (1984) 93-101.
[48] A.S. Cordeiro, J. Crecente-Campo, B.L. Bouzo, S.F. González, M. de la Fuente, M.J. Alonso, Engineering polymeric nanocapsules for an efficient drainage and biodistribution in the lymphatic system, Journal of drug targeting, (2019) 1-13.
[49] V. Manolova, A. Flace, M. Bauer, K. Schwarz, P. Saudan, M.F. Bachmann, Nanoparticles target distinct dendritic cell populations according to their size, European journal of immunology, 38 (2008) 1404-1413.

Tables

Table 1. Summary of cationic liposome formulations used in *in vitro* and *in vivo* studies. All liposomes were formulated at 4 mg/mL lipid concentration, 1:1 flow rate ratio and 15 mL/min total flow rate. Small liposomes were formulated at 10 mM TRIS buffer pH 7.4. Large DOPE:DOTAP and large DOPE:DDA liposomes were formulated at 1000 and 300 mM TRIS buffer pH 7.4 respectively. For *in vivo* studies, all formulations were adjusted 10% trehalose for isontonicity. Results are represented as mean ± SD of three independent experiments.

Formulation	Size (d.nm)	PDI	Zeta-potential (mV)
Small DOPE:DOTAP	44 ± 5	0.215 ± 0.045	42 ± 5
Large DOPE:DOTAP	754 ± 67	0.145 ± 0.070	50 ± 4
Small DOPE:DDA	41 ± 8	0.193 ± 0.031	61 ± 6
Large DOPE:DDA	481 ± 42	0.232 ± 0.064	61 ± 2

Figure Legends

Figure 1. Schematic representation of the microfluidic formulation of small **(A)** and large **(B)** unilamellar liposomes (SUV and LUV). Small (40 nm) and large (>500 nm) liposomes were formulated by microfluidics in the Nanoassemblr Platform at 4 mg/mL, 1:1 FRR and 15 mL/min TFR at either 10 or higher TRIS concentration. Solvent removal and buffer exchange was undertaken via dialysis against 10 mM TRIS (200 mL) for 1 hour under magnetic stirring to adjust buffer concentration. The concentration of buffer and lipid selection offer controlled production of large uni/oligolamellar vesicles.

Figure 2. The effect of aqueous buffer concentration on liposomes formulated by microfluidics. Effect of cationic lipid choice. DOPE:DOTAP (●), DOPE:DDA (▣) and DSPC:Chol (△) liposomes were formulated by microfluidics in the Nanoassemblr Platform (Precision Nanosystems) at increasing concentrations of TRIS buffer pH 7.4, then dialyzed and characterized by dynamic light scattering in terms of size **(A)**, PDI **(B)** and zeta-potential **(C)**. Dynamic light scattering size distribution plots of DOPE:DOTAP **(D)**, DOPE:DDA **(E)** and DSPC:Chol **(F)** liposomes, and representative images of formulations prepared at lowest (left) and highest (right) buffer concentration are shown. Results are represented as mean ± SD of three independent experiments.

Figure 3. Cryo-TEM micrographs of small **(A, B)** and large DOPE:DOTAP liposomes **(D , E)** formulated by microfluidics at 4 mg/mL, 1:1 FRR, 15 mL/min TFR and 10 and 1000 mM TRIS buffer pH 7.4. The dense black spheres are water crystals. Hydrodynamic size (bars) and PDI (values) **(F)** and size distribution plots of small and large liposomes **(G)** are shown. Results are represented as mean ± SD of three DLS measurements.

Figure 4. The role of cationic lipid content within the liposome formulation. Effect of molar percentage of cationic lipid on size **(A)**, PDI **(B)** and zeta-potential **(C)**. DSPC:Chol liposomes (10:10 molar ratio) were prepared at increasing molar percentages of DOTAP: 0% (●), 5% (▣), 13% (△) and 23% (◇). All formulations were prepared at 4 mg/mL, 1:1 FRR and 15 mL/min TFR, dialyzed and characterized by DLS. Effect of buffer choice on size **(D)** and PDI **(E)**. DSPC:Chol (10:10 molar ratio) and DSPC:Chol:DOTAP (10:10:1 molar ratio) liposomes were prepared at 4 mg/mL, 1:1 FRR and 15 mL/min at increasing concentrations of TRIS buffer pH 7.4 or citrate buffer pH 6.0, dialyzed and characterized by DLS. DSPC:Chol – TRIS buffer (●), DSPC:Chol – citrate buffer (▣), DSPC:Chol:DOTAP – TRIS buffer (△), DSPC:Chol:DOTAP – Citrate buffer (◇). Results are represented as mean ± SD of three independent experiments.

Figure 5. Liposome-cell interactions in bone marrow-derived macrophages *in vitro*. **A)** Percentage of liposome$^+$ or Dil-C_{18}^+ cells (surface-associated or internalized). **B)** Mean Fluorescence Intensity (MFI) **C)** Relative liposome surface area (SA_r). **D)** Relative number of liposomes (N_r). **E)** Relative liposome internal volume (V_r). Small DOPE:DOTAP (□), small DOPE:DDA (□), large DOPE:DOTAP (■), large DOPE:DDA (■). **F)** Representative flow cytometry plots of liposome uptake at 1, 4 and 24 hours (black) with respect to control cells at time zero (shaded grey). Results are represented as mean ± SD of three independent experiments. Statistical analysis was performed by one-way ANOVA followed by Turkey test. $P<0.05$ (*), ns (non-significant).

Figure 6. *In vivo* biodistribution of small (-●-) and large (··○··) DOPE:DOTAP **(A – C)** and DOPE:DDA **(D – E)** cationic liposomes in CD1 mice upon intramuscular injection. The percentage of injected dose was analysed at the injection site **(A, D)**, popliteal lymph node **(B, E)** and inguinal lymph node **(C, F)**. Results are represented as mean ± SD of 4 ± 1 mice. **G)** AUC for each of the sites considered.

Low ionic strength

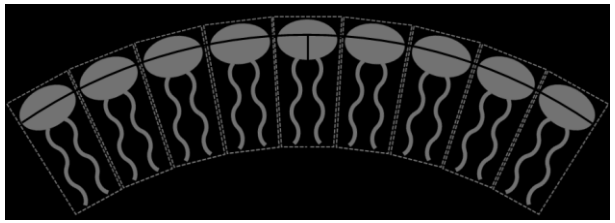

r1 (small liposome)

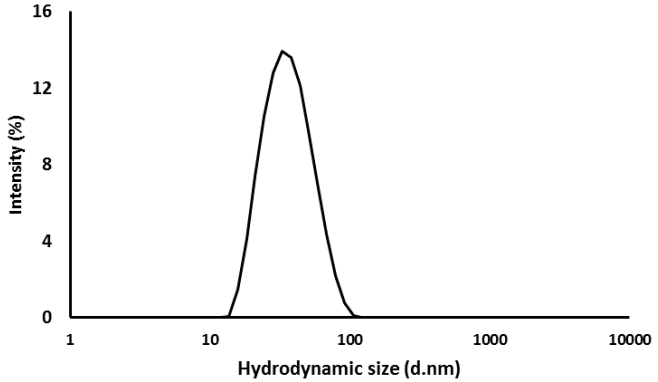

High ionic strength

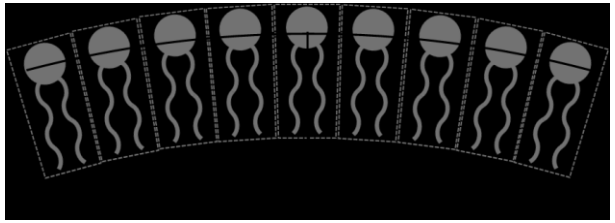

r2 (large liposome)

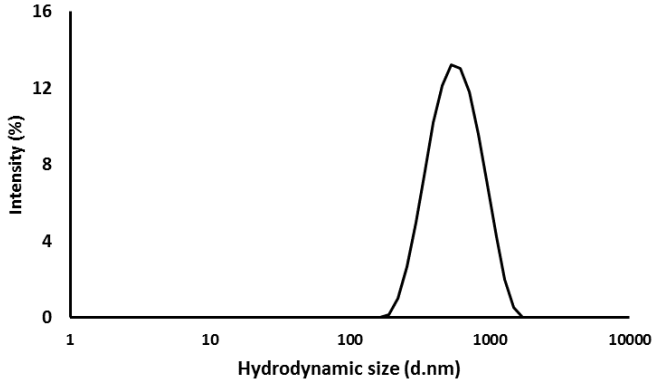

Graphical abstract

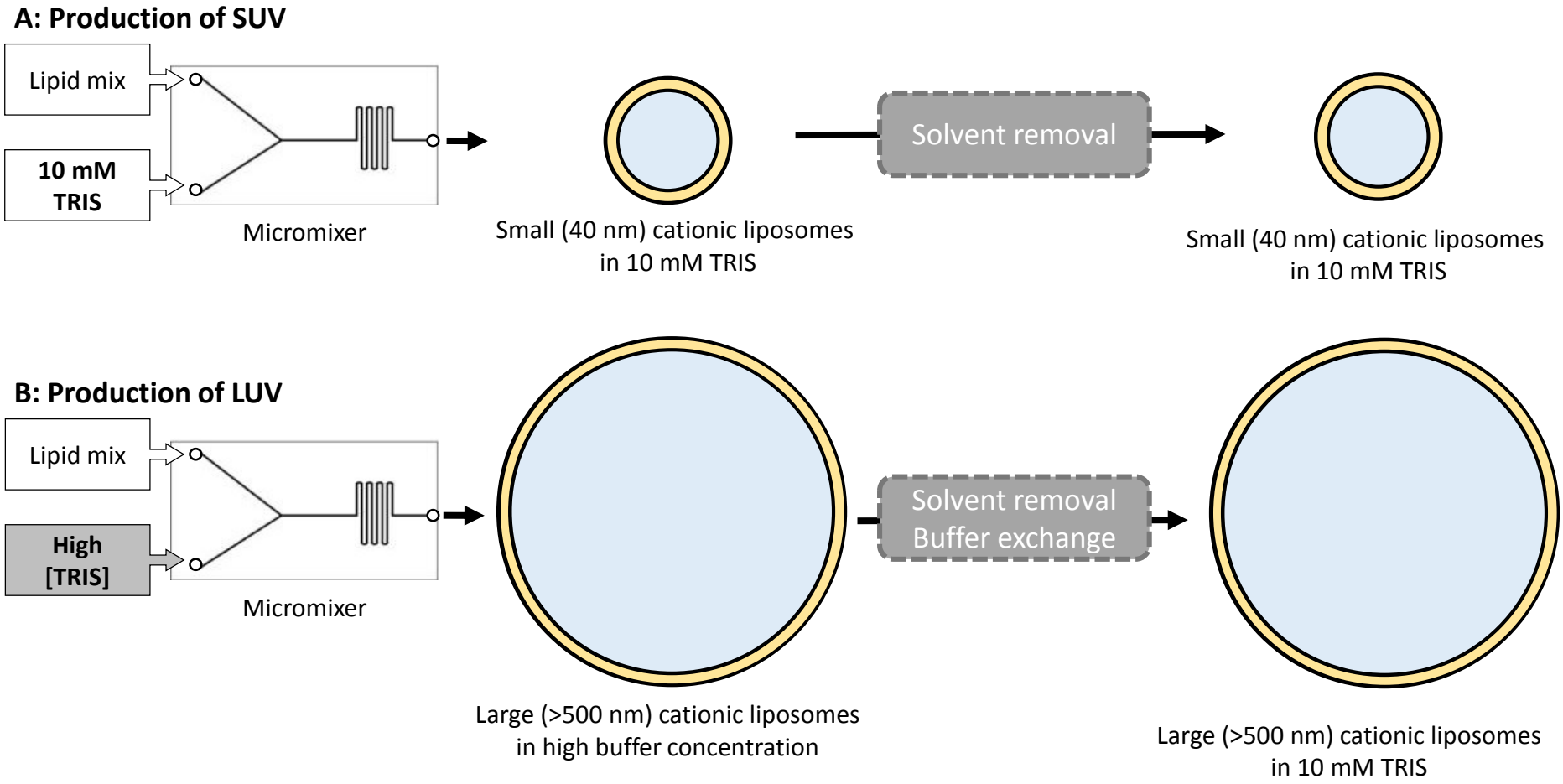
A: Production of SUV
Lipid mix
10 mM TRIS
Micromixer
Small (40 nm) cationic liposomes in 10 mM TRIS
Solvent removal
Small (40 nm) cationic liposomes in 10 mM TRIS
B: Production of LUV
Lipid mix
High [TRIS]
Micromixer
Large (>500 nm) cationic liposomes in high buffer concentration
Solvent removal
Buffer exchange
Large (>500 nm) cationic liposomes in 10 mM TRIS

Figure 1

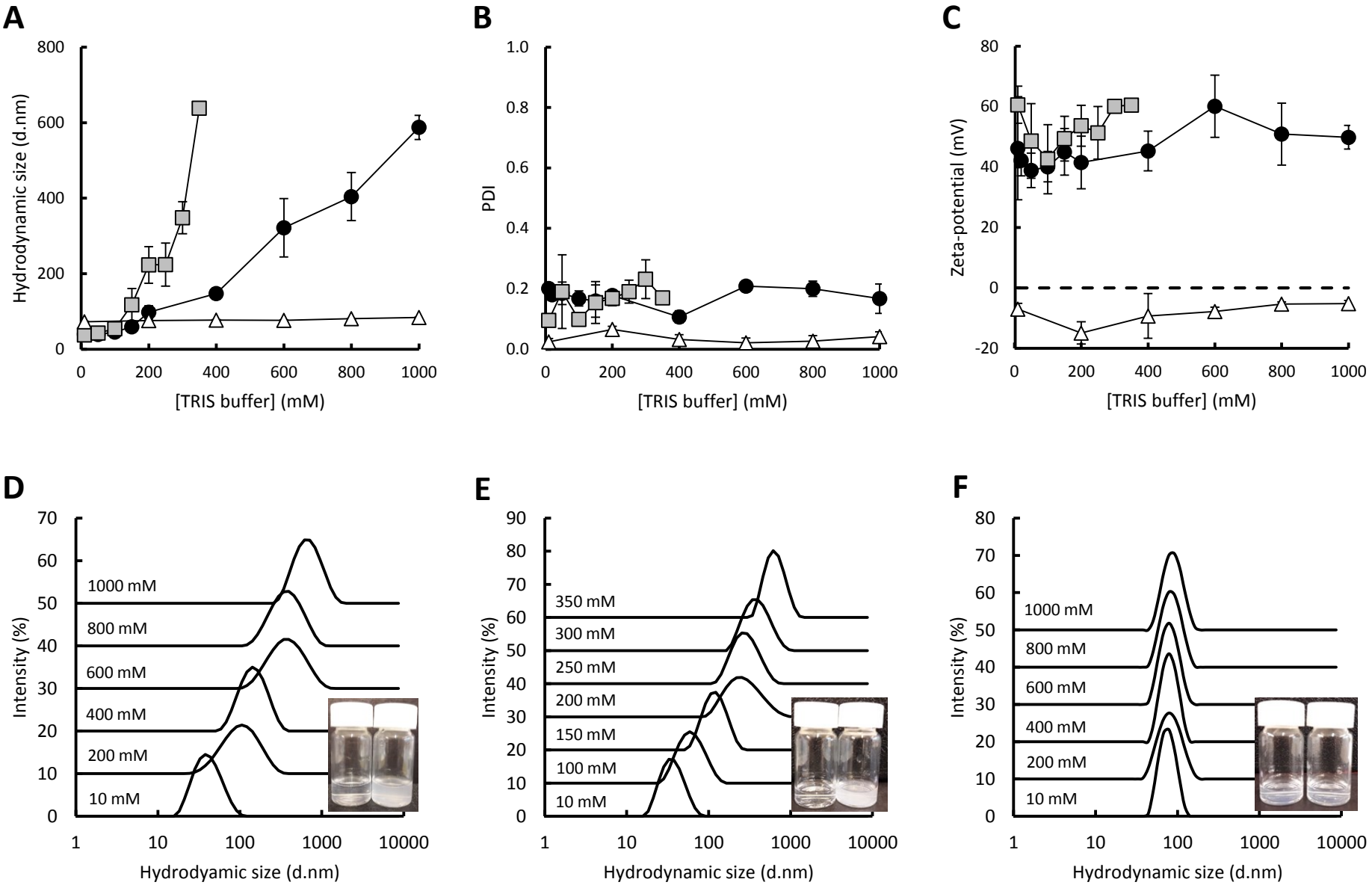
A
Hydrodynamic size (d.nm)
[TRIS buffer] (mM)
B
PDI
[TRIS buffer] (mM)
C
Zeta-potential (mV)
[TRIS buffer] (mM)
D
Intensity (%)
1000 mM
800 mM
600 mM
400 mM
200 mM
10 mM
Hydrodyamic size (d.nm)
E
Intensity (%)
350 mM
300 mM
250 mM
200 mM
150 mM
100 mM
10 mM
Hydrodynamic size (d.nm)
F
Intensity (%)
1000 mM
800 mM
600 mM
400 mM
200 mM
10 mM
Hydrodynamic size (d.nm)

Figure 2

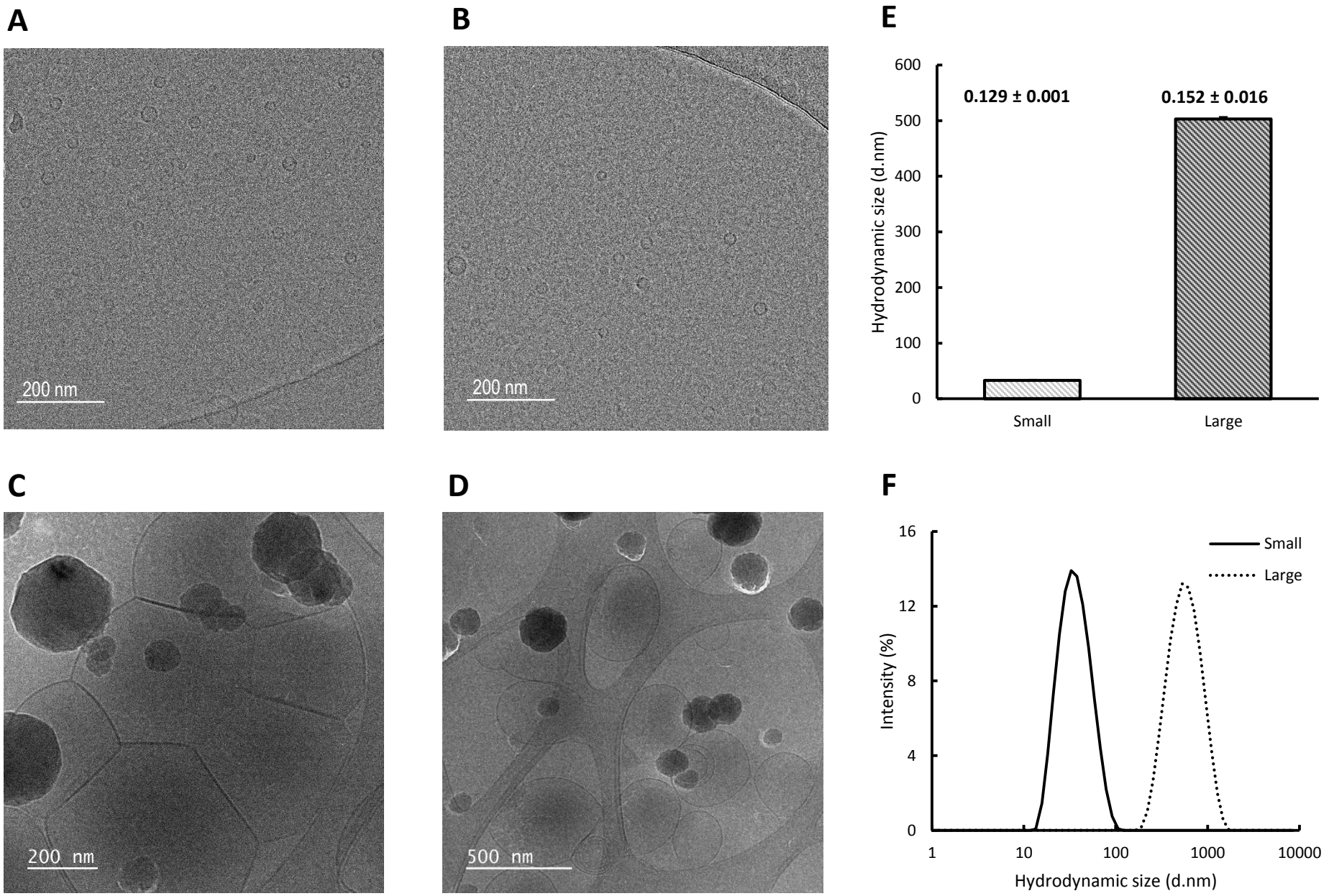
A
200 nm
B
200 nm
E
600
500
400
300
200
100
0
Hydrodynamic size (d.nm)
0.129 ± 0.001
0.152 ± 0.016
Small
Large
C
200 nm
D
500 nm
F
16
12
8
4
0
Intensity (%)
Small
Large
1
10
100
1000
10000
Hydrodynamic size (d.nm)

Figure 3

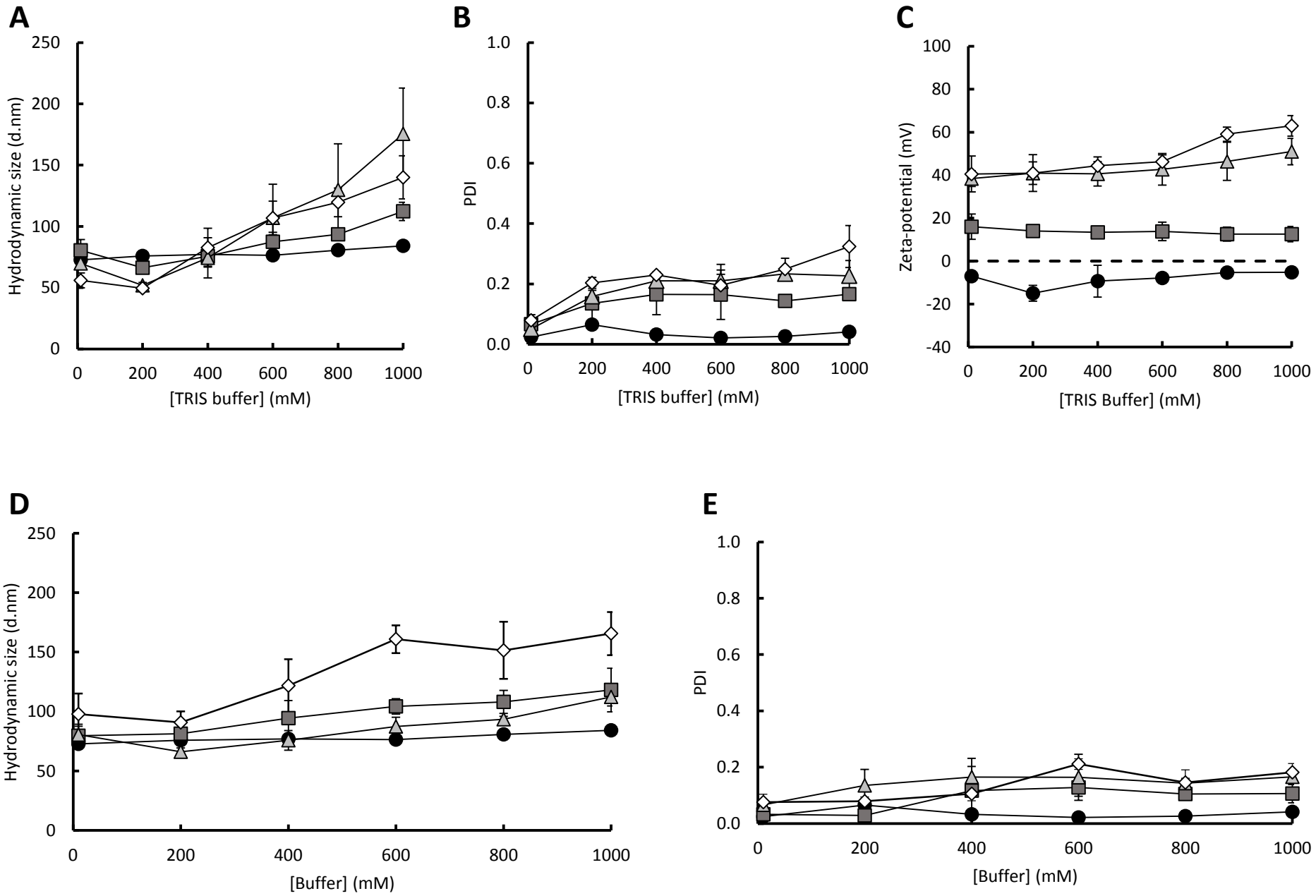
A
Hydrodynamic size (d.nm)
250
200
150
100
50
0
0
200
400
600
800
1000
[TRIS buffer] (mM)
B
PDI
1.0
0.8
0.6
0.4
0.2
0.0
0
200
400
600
800
1000
[TRIS buffer] (mM)
C
Zeta-potential (mV)
100
80
60
40
20
0
-20
-40
0
200
400
600
800
1000
[TRIS Buffer] (mM)
D
Hydrodynamic size (d.nm)
250
200
150
100
50
0
0
200
400
600
800
1000
[Buffer] (mM)
E
PDI
1.0
0.8
0.6
0.4
0.2
0.0
0
200
400
600
800
1000
[Buffer] (mM)

Figure 4

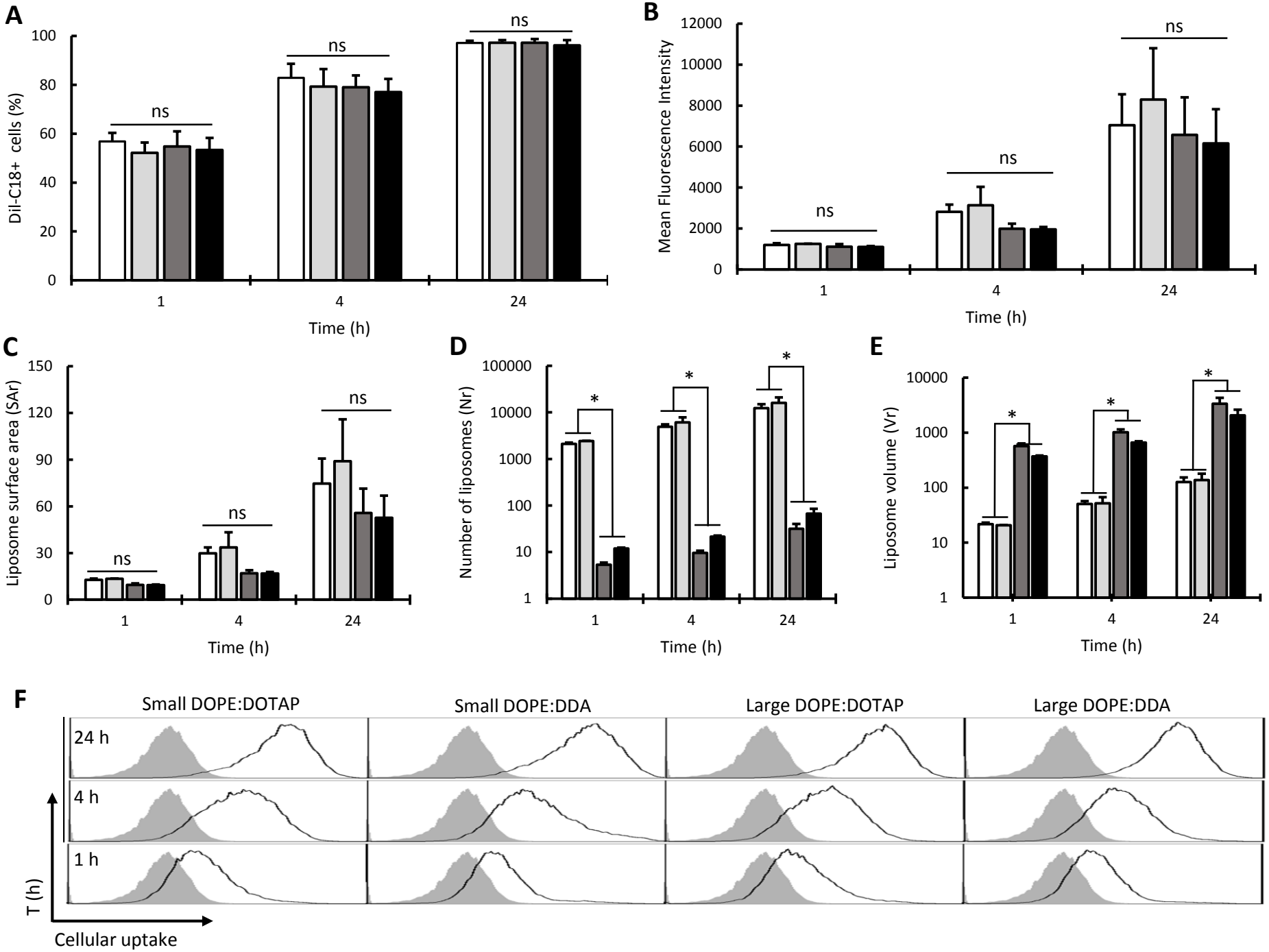
A
Dil-C18+ cells (%)
100
80
60
40
20
0
ns
ns
ns
1
4
24
Time (h)
B
Mean Fluorescence Intensity
12000
10000
8000
6000
4000
2000
0
ns
ns
ns
1
4
24
Time (h)
C
Liposome surface area (SAr)
150
120
90
60
30
0
ns
ns
ns
1
4
24
Time (h)
D
Number of liposomes (Nr)
100000
10000
1000
100
10
1
*
*
*
1
4
24
Time (h)
E
Liposome volume (Vr)
10000
1000
100
10
1
*
*
*
1
4
24
Time (h)
F
Small DOPE:DOTAP
Small DOPE:DDA
Large DOPE:DOTAP
Large DOPE:DDA
24 h
4 h
1 h
T (h)
Cellular uptake

Figure 5

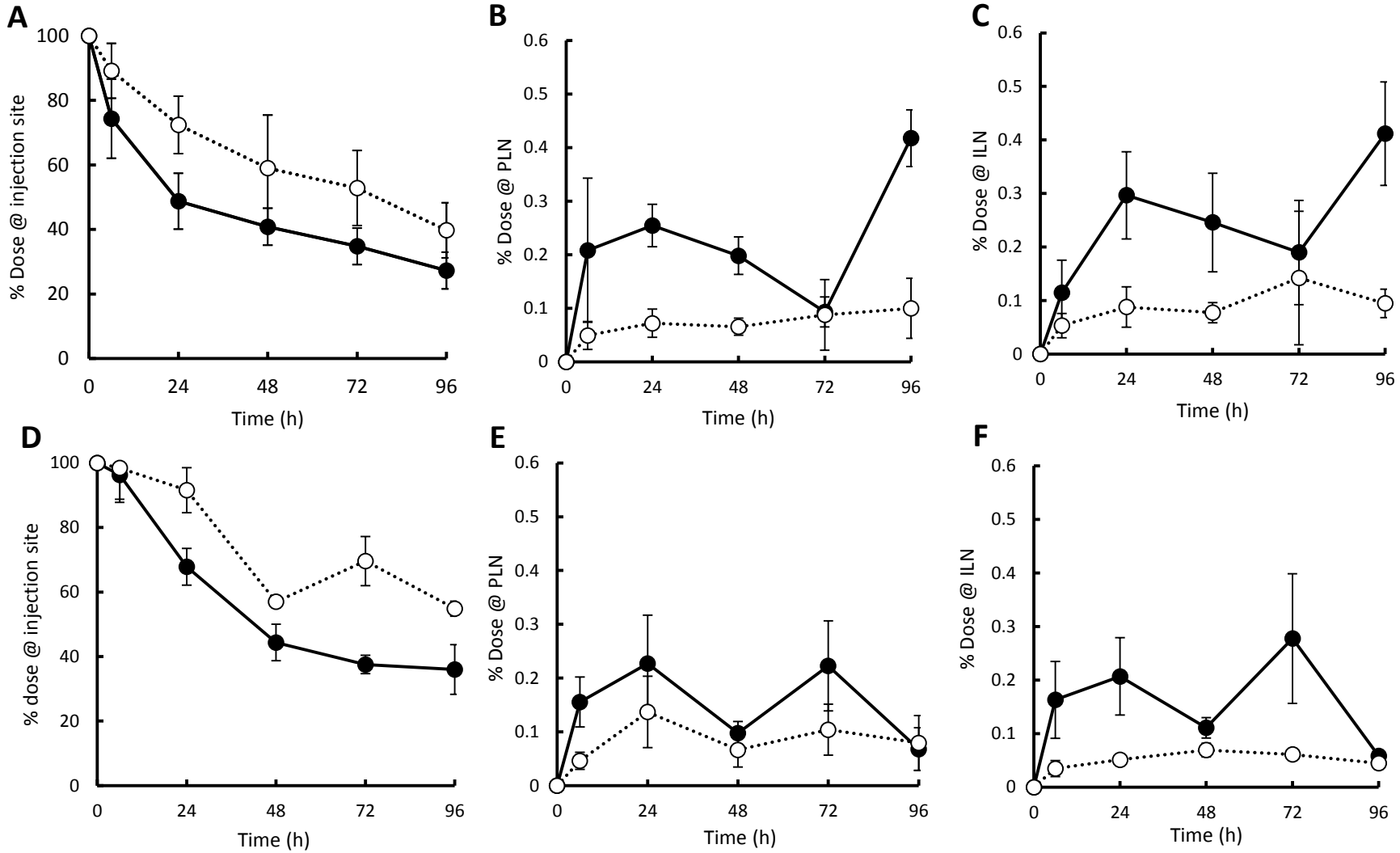

G	AUC (%Dose.h)		
Formulation	**Injection site**	**PLN**	**ILN**
Small DOPE:DOTAP	3847 ± 279	19 ± 2	24 ± 5
Large DOPE:DOTAP	5462 ± 972	7 ± 2	10 ± 4
Small DOPE:DDA	4689 ± 307	13 ± 2	15 ± 4
Large DOPE:DDA	6402 ± 399	8 ± 2	5 ± 0.2

Figure 6

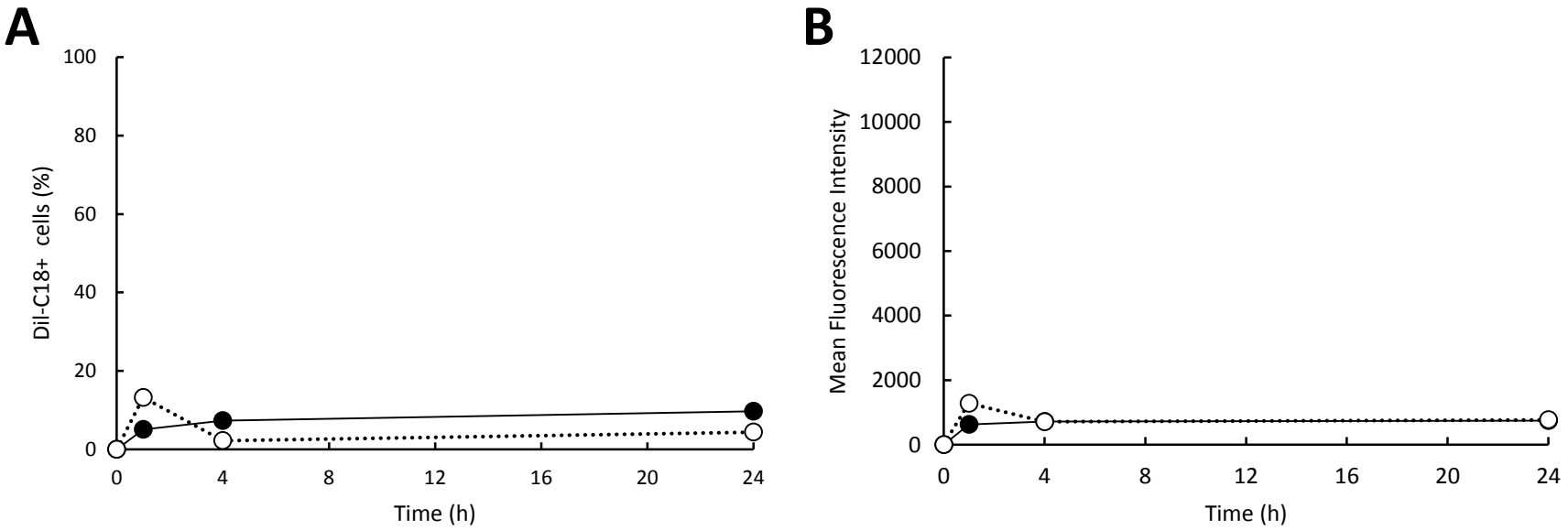

Figure S1. Cationic liposome-cell interactions in bone marrow-derived macrophages (BMDM) at 4 °C *in vitro* in terms of Dil-C18+ cells **(A)** and Mean Fluorescence Intensity **(B)**. Replicate 1 (black circle), replicate 2 (white circle).

Figure S1